

Rocking Newton's cradle

Stefan Hutzler, Gary Delaney,^{a)} Denis Weaire, and Finn MacLeod

Physics Department, Trinity College Dublin, Dublin 2, Ireland

(Received 15 December 2003; accepted 25 June 2004)

In textbook descriptions of Newton's cradle, it is generally claimed that displacing one ball will result in a collision that leads to another ball being ejected from the line, with all others remaining motionless. Hermann and Schmälzle, Hinch and Saint-Jean, and others have shown that a realistic description is more subtle. We present a simulation of Newton's cradle that reproduces the break-up of the line of balls at the first collision, the eventual movement of all the balls in phase, and is in good agreement with our experimentally obtained data. The first effect is due to the finite elastic response of the balls, and the second is a result of viscoelastic dissipation in the impacts. We also analyze a dissipation-free ideal Newton's cradle which displays complex dynamics. © 2004 American

Association of Physics Teachers.

[DOI: 10.1119/1.1783898]

I. INTRODUCTION

A line of touching balls suspended from a rail by pairs of inelastic strings is often called Newton's cradle (see Fig. 1). In introductory physics textbooks,¹⁻⁶ it is generally introduced as an illustration of the conservation of momentum and energy. When one ball is displaced from the other four and released, it is claimed that the collisions will result in the ball at the opposite end of the line being ejected, with all other balls remaining stationary. As the ejected ball swings back, it will collide with the line of balls. According to the common description, only the ball that was released initially will be ejected, while all other balls remain stationary.

However, the actual experiment reveals a slightly different scenario. Careful observation shows that the first collision will break up the line of balls with the effect that all balls move. After further collisions all balls will eventually swing in phase, with an ever decreasing amplitude. The observed breakup of a line of balls after the impact of one ball was analyzed recently by Hinch and Saint-Jean.⁷ We extend their work to consider the multiple collisions that follow thereafter. We believe that a closer examination of Newton's cradle can enhance and extend the pedagogical value of the original demonstration.⁸⁻¹⁰

Newton's cradle has a long history. In 1662, papers on its underlying physics were presented to the Royal Society by no less than three eminent researchers,⁵ John Wallis (known for his presentation of π as an infinite product), Christopher Wren (mathematician, astronomer and architect of St. Paul's Cathedral in London), and Christiaan Huygens (author of a book on the wave theory of light and contributions to probability theory). Huygens pointed out that an explanation required both conservation of momentum and kinetic energy. (He did not use the expression kinetic energy but referred to a quantity proportional to mass and velocity squared.)

However, two equations are not sufficient to describe the behavior of Newton's cradle as was pointed out in Ref. 8. A characterization of Newton's cradle consisting of N balls requires N velocities, but the conservation laws only give two equations. Herrmann and Schmälzle⁸ analyzed Newton's cradle in terms of elastic forces between the contacting balls. They argued that a necessary condition for consistency with the simplified textbook description is that there be no dispersion in the relation between frequency and wave number for

the vibrational motion of the chain of contacting balls. Their conclusion was based on their experiments with gliders on an air track, where each glider was equipped with a spring bumper. These experiments effectively model the first set of collisions in Newton's cradle. When all gliders are in contact, the gliders may be represented as a linear chain, allowing for the calculation of eigenfrequencies and corresponding wave numbers. Only when the masses of the gliders and the spring constants were chosen to achieve a dispersion-free linear relation, did the gliders behave as in the textbook description.^{8,10}

In a follow-up paper, Herrmann and Seitz⁹ re-examined the actual cradle experiment and found in both the experiments and simulations that the first impact of a ball leads to a break-up of the line, contrary to the textbook description. In their simulations, they modeled the interaction between balls as points of mass m that are connected by (Hertzian) springs. The force between two such masses is given by

$$F = k(y_n - y_{n-1})^\alpha, \quad (1)$$

where y_n is the displacement of ball n from its equilibrium position, k is a spring constant, and the exponent $\alpha = 3/2$. The comparison of the propagation time of a perturbation through a line of balls obtained from both experiments and simulations using a range of different values of α showed that the assumption of Hertzian springs in Eq. (1) is valid. From their simulations of a five-ball cradle, Herrmann and Seitz found that after the first collision, balls 1, 2, and 3 move backward, while balls 4 and 5 move forward with ball 4 carrying about 12% of the initial momentum of the incident ball. [We have labeled the balls in the direction from the incoming ball (ball 1) to the ball at the opposite end of the line (ball 5).] The momentum of ball 5 after the collision is nearly as large as that of ball 1 before the collision.

Without performing further simulations Herrmann and Seitz⁹ concluded that when ejected ball 5 swings back, it would impact not on a compact line of balls (because the line has been broken up by the first impact), but rather there should be a sequence of independent collisions. However, in general, there can be multiple collisions involving more than two balls in contact during the collision as we will see in Sec. II. This issue will be examined further in relation to our experimental results discussed in Sec. VI.

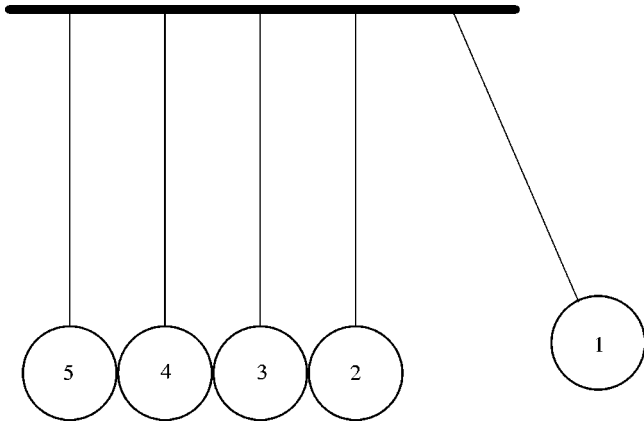


Fig. 1. Newton's cradle. Ball 1 on the right is released and swings down to impact the line of stationary balls. It is generally suggested that only ball 5 on the left is ejected. However, both experiments and our simulations show that all balls will move after the impact.

Hinch and Saint-Jean⁷ conducted an exhaustive numerical and theoretical study of the fragmentation of a line of N balls by an impact. They find that some balls at the far end detach from the line and fly off, some in the middle hardly move, and the impacting ball rebounds backward bringing with it some of its nearby balls. They reproduced the numerical results of Ref. 9 for the first impact, and also set their results into a wider context. For a linear contact force law ($\alpha = 1$), the number of balls that are detached from the line is

$$N_{\text{detach}} = 1.5N^{1/3}, \quad (2)$$

while the majority of balls rebound. For the Hertzian force law ($\alpha = 3/2$) only a few balls rebound together with the impacting ball, with a velocity greater than 1% of the impact velocity. For example, for a line of $N = 5$ balls, two balls will leave in the forward direction, for $N = 15$ this number increases to three. However, no power law analogous to Eq. (2) was established.

Despite the above studies and recent work in engineering literature,¹¹ there still is a need for further work on the nature of Newton's cradle for the following reasons. Because gravity was not included, the discussion was limited to the first impact. What happens in subsequent collisions? If we assume a dissipation-free system, will the motion settle down to a regular behavior or will it be chaotic? In what way will dissipation affect the motion? We will discuss these questions by presenting the results of theory, experiments, and simulations where gravity has explicitly been included, together with dissipative effects due to collisions and friction. Our work by no means exhausts the possible corrections that might be added to the model, but it seems sufficient for the available data.

II. MODELING NEWTON'S CRADLE

We define the overlap $\xi_{m,n}$ between two balls m and n as

$$\xi_{m,n} = (2R - r_{mn})_+, \quad (3)$$

where R is the radius of the balls and r_{mn} is the distance between their centers (see Fig. 2). The notation $()_+$ specifies that the value of the bracket is zero if the expression inside is negative, as required for the representation of contact forces that cannot be in tension. If we model the contact forces as

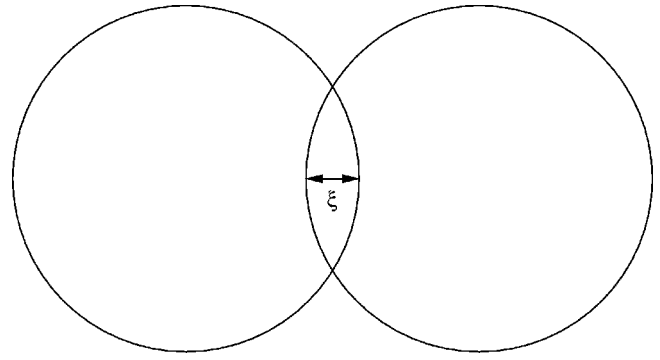


Fig. 2. The overlap of two balls.

described in Sec. I, the force on ball n may be written as

$$m\ddot{x}_n = k[\xi_{n-1,n}^\alpha - \xi_{n,n+1}^\alpha], \quad (4)$$

where x_n denotes the position of ball n .

The introduction of gravity requires some discussion. Although Eq. (4) holds for a one-dimensional line of balls where the impact is in the same direction as the line, Newton's cradle is two dimensional. The balls are attached to a frame by an inelastic string of length L and can swing about their respective equilibrium positions $(x_{o,n}, L)$ along arcs of circles. This motion causes the collisions to become off centered if the balls are a finite distance away from their equilibrium positions. Our model neglects this effect. It is restricted to small angles or amplitudes $|x_n - x_{o,n}| \ll L$, in order to maintain a one-dimensional description of the cradle.

In the same approximation, gravity can be modeled as a simple restoring force, that is, a harmonic spring which acts to move each ball back to its equilibrium positions $x_{o,n}$. The gravitational spring constant is given by $k_g = mg/L$.

The equations of motion for the dissipation-free Newton's cradle are thus:

$$m\ddot{x}_n = k\xi_{n-1,n}^\alpha - k\xi_{n,n+1}^\alpha + k_g(x_{o,n} - x_n), \quad (5)$$

where n ranges from 1 to N . We solved Eq. (5) for $N = 5$ using the second-order velocity Verlet algorithm¹² and the initial conditions for $x_n(t=0)$: $x_1(0) = A$, $x_n(0) = x_{o,n}$ for $2 \leq n \leq 5$, and $\dot{x}_n(0) = 0$ for all n , corresponding to one ball being released with an amplitude A on to a stationary line of balls (see Fig. 1).

Modeling contacting spheres requires $\alpha = 3/2$ (Hertz law).¹³ The spring constant k may be written in terms of material constants as

$$k = \sqrt{2RE}/[3(1-\nu^2)], \quad (6)$$

where E is Young's modulus, ν is Poisson's ratio, and R is the radius of the balls.⁷

It is common to introduce dimensionless variables before solving the equations of motion numerically. However, in our problem there are two time and length scales. Although the swinging balls may best be described in terms of their period $T_0 = 2\pi\sqrt{L/g}$ and string length L , individual collisions occur on a much shorter time scale $t_0 = (m^2/k^2v)^{1/5}$ and displacement scale $l_0 = (m^2v^4/k^2)^{1/5}$. Here, v is the velocity of the impacting ball, given by $v = A\sqrt{g/L}$.

Because Eq. (5) describes a conservative system, the appropriate time step Δt for the numerical integration may be

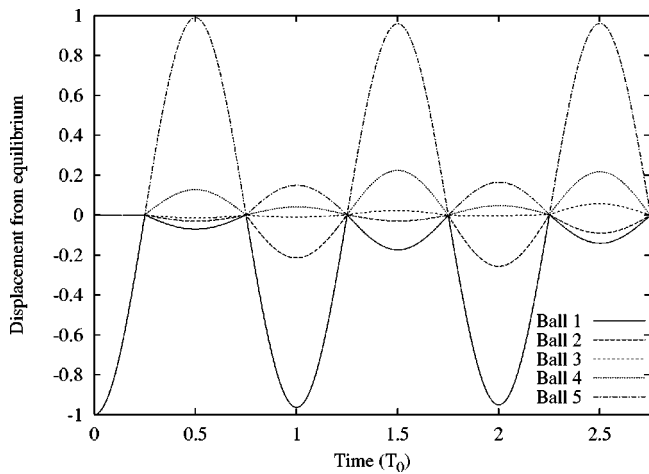


Fig. 3. Displacement from their respective equilibrium positions of each of the five balls as a function of time. Note that the first impact results in a fragmentation of the line of balls. Contrary to textbook explanations of Newton's cradle, all balls are subsequently in motion. In the early stages of this dissipation-free simulation, the largest amplitudes of motion are exhibited by balls 1 and 5. (The displacement is plotted as a fraction of the initial amplitude of the incident ball. Time is displayed in multiples of the period of a single ball $T_0 = 2\pi\sqrt{L/g}$.)

found by checking for energy conservation. Our chosen time step of approximately $2.5 \times 10^{-3} t_0$ lead to a relative error in the energy of not more than 0.005% over a time of over $10\,000 T_0$.

An initial test of our code was undertaken by setting $k_g = 0$ to model the impact on a line of balls in the absence of gravity. This simulation reproduced the results of Ref. 7 for the final velocities of all balls after the impact.

III. RESULTS

For $k_g > 0$, we found that the first collision breaks up the line of balls. As the balls move back toward their respective equilibrium positions, however, they do not return to their individual stationary starting positions. This difference leads to a different scenario for the second set of collisions. As

time evolves, an oscillatory motion becomes established, as we will demonstrate in Sec. IV for the case of $N=2$.

Figure 3 shows the displacements of the balls for $N=5$ where ball 1 has been released from an amplitude $A = 0.27L$ onto a line of four balls. The collision (at time $\pi/2\sqrt{L/g}$) results in the break-up of the line with balls 4 and 5 moving forward and balls 1, 2, and 3 rebounding. Ball 5 reaches its maximum displacement at time $\pi\sqrt{L/g}$. As it swings back, it will no longer hit a stationary line at time $3\pi/2\sqrt{L/g}$. The second set of collisions, shown in Fig. 4(b) is thus not antisymmetric to the first set [see Fig. 4(a)]. Figure 4(c) displays the third set of collisions, which is clearly different from the first set.

Due to the fragmentation of the line of balls at the initial collision, there are no obvious symmetry considerations that can explain the configurations in the latter collisions. The question arises as to whether the system of five balls will develop any periodicity in its long-term behavior or will be chaotic. Our data for a time of more than $10\,000 T_0$ is best displayed by showing phase portraits at various times (see Fig. 5). Generally, there is one ball colliding with a line of four slightly separated balls. However, the amplitudes of the first ball and the line of balls display very low-frequency oscillations between two modes of motion. In mode I, the cluster of four balls moves much slower than the single ball, while in mode II all balls move with a similar speed.

This behavior is particularly pronounced for $N=2$, but also is well pronounced for $N=4$ and $N=5$ as shown in Fig. 5.

IV. THEORY OF A TWO-BALL CRADLE

We now present an analytical treatment of the relatively simple two-ball cradle, which leads to the identification of the behavior with the phenomenon of beats. We will show that the softness of the balls leads to an oscillation of the collision points. This variation of the phase portrait in time is also seen in our simulations of the three- and four-ball cradles.

Even if the balls are not infinitely hard, the standard textbook description is still valid in the sense that the impacting ball comes to a complete standstill while the impacted ball

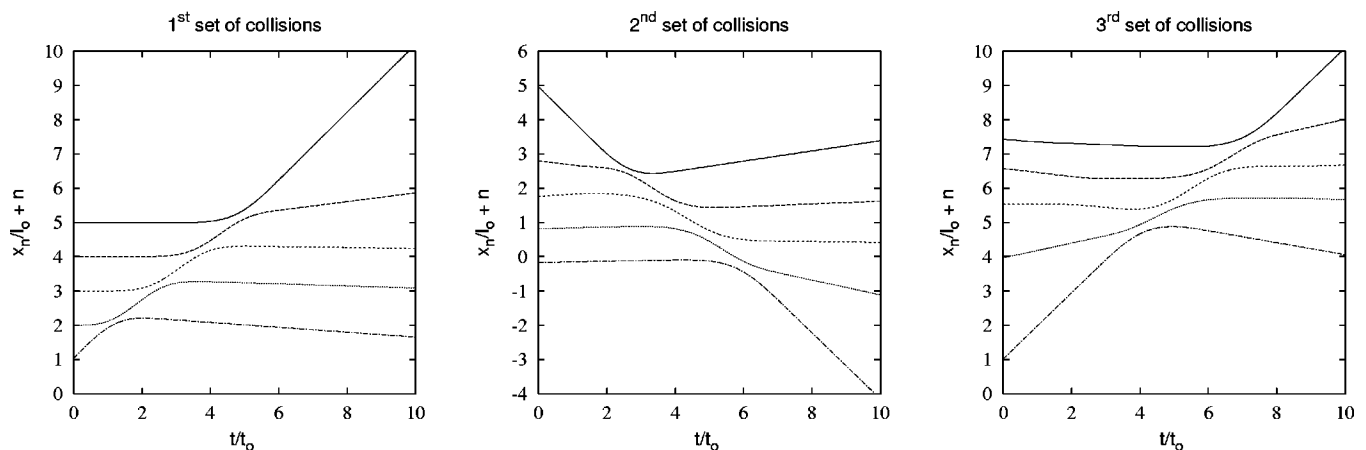


Fig. 4. A detailed view of the first three sets of collisions reveals the symmetry breaking that occurs due to the break-up of the line in the first collision. Time is displayed in multiples of $(m^2/k^2v)^{1/5}$. We have chosen the time origin as the moment when the incident ball passes through its equilibrium position. The displacements are made dimensionless by dividing by the length scale l_0 . For visual clarity, they are shifted by n , where the balls are labeled from 1 to 5 as in Fig. 1.

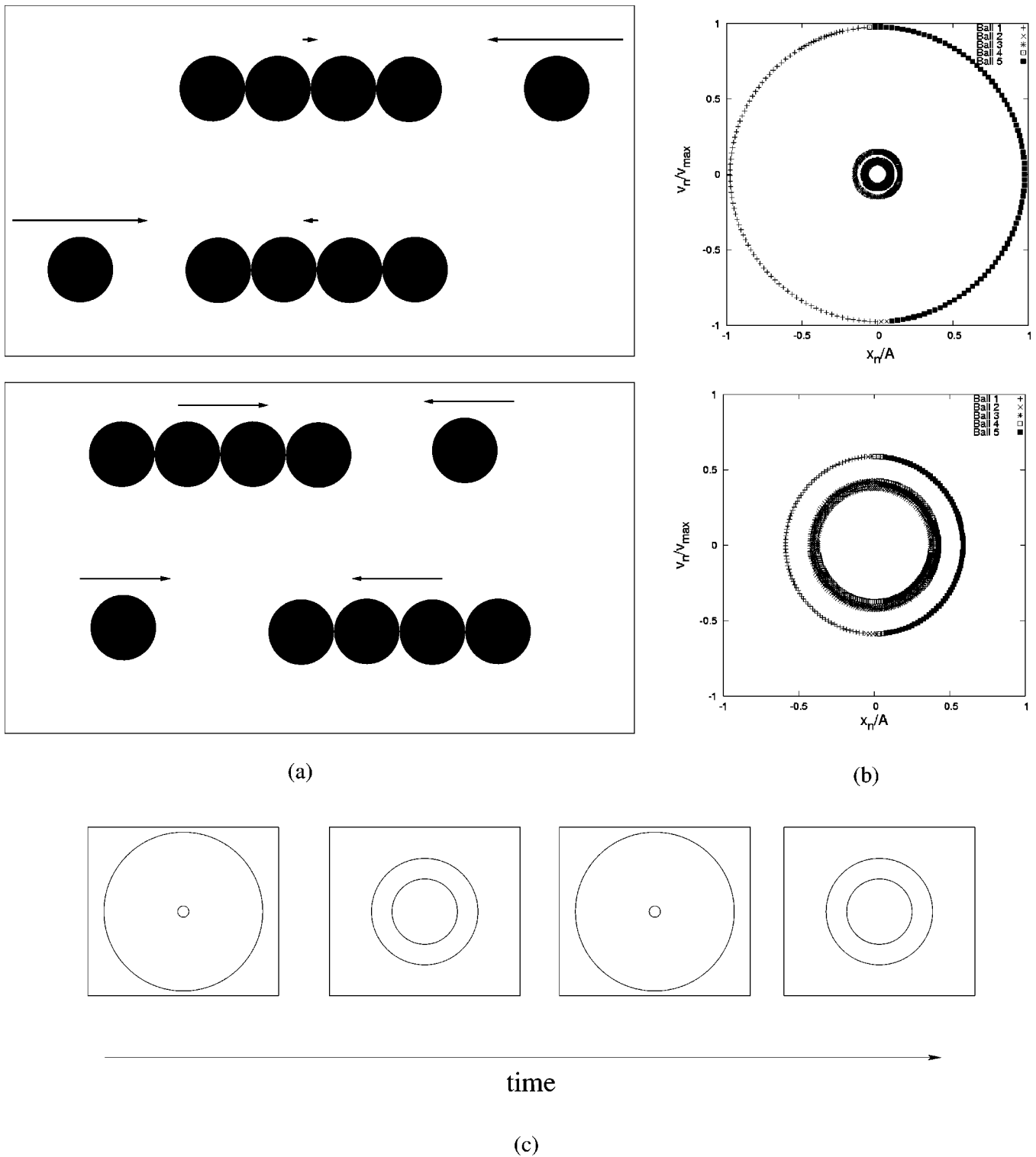


Fig. 5. (a) The long-time behavior of the dissipation-free $N=5$ cradle is characterized by a slow oscillation between two modes of motion. Both modes involve the collision of one ball against a group of four. In mode II all balls move with a similar speed, in mode I the cluster moves much slower than the single ball. (b) Simulation results in the form of phase portraits. (c) A sketch of the evolution of these portraits.

moves off with the same velocity as the impacting ball. However, what is generally ignored is the fact that the impact does not take place instantaneously. During this finite interaction time, both balls have a nonzero velocity and their point of contact will move a certain distance along the direction of the impact. (For a discussion of the related case of a

bullet shot into a hanging block, see Ref. 14.) The impacted ball will move away from its equilibrium position by a distance Δx and will consequently swing back after the collision. From our simulations, we find that Δx scales as $\Delta x \propto m^{5/2} v^{5/4} k^{-2/5}$, consistent with the displacement scale introduced in Ref. 7.¹⁵

The subsequent behavior, sketched in Sec. III, can be analyzed as follows. If we denote the positions of each ball relative to their respective equilibrium position by x_1 and x_2 , the center of mass X_c is given by

$$X_c = \frac{(x_1 + x_2)}{2}, \quad (7)$$

while the relative position X_r is

$$X_r = x_1 - x_2. \quad (8)$$

For simplicity, we shall assume a harmonic force law (with spring constant K_r), where the subscript r signifies that the interaction is due to the relative positions of the balls. The validity of the argument will however not be restricted to this force law. The cradle will be seen to be equivalent to a pair of coupled oscillators that are coupled only when the two balls are in contact ($X_r > 0$).

Each ball is subject to gravitation, modeled as a spring with spring constant $K_c = mg/L$, as in Sec. II. (Previously, this constant was called k_g , but we shall use K_c in the following discussion to remind us that the spring acts on the center of gravity of the two balls.) The potential energy of each ball is given by $\frac{1}{2}K_c X_c^2$. The potential energy of contact is given by $\frac{1}{2}K_r X_r^2$ for $X_r > 0$ and is zero for $X_r \leq 0$. The natural frequencies associated with the two spring constants for mass m are given by $\Omega^2 = K_c/m$ and $\omega^2 = K_r/m$.

We consider the case where ball 1 is released from $x_1 = -A$ and $x_2 = 0$. Then initially we have

$$X_c = \frac{x_1 + x_2}{2} = -A, \quad (9a)$$

$$X_r = -A. \quad (9b)$$

The center of mass motion is that of a mass $2m$ acted on by external forces ($F = -K_c X_c$) only. Hence, the motion is simple harmonic with frequency Ω :

$$X_c = -\frac{A}{2} \cos \Omega t. \quad (10)$$

The dependence of the relative position X_r on the time as obtained from our simulation is shown in Fig. 6.

The cradle features two time scales, the collision time, τ_0 and the time between collisions, $\Gamma_0 \gg \tau_0$, given by

$$2\Gamma_0 = \frac{2\pi}{\Omega}, \quad (11)$$

corresponding to free motion under the action of K_c with $X_r \leq 0$.

We make the approximation that during a collision ($X_r > 0$), where the repulsive force due to K_r dominates, we neglect K_c . Then, the motion is another (short) half-cycle under K_r , as is seen in Fig. 6. We find for the interaction time τ_0

$$2\tau_0 = \frac{2\pi}{\sqrt{2}\omega} = \frac{\sqrt{2}\pi}{\omega}. \quad (12)$$

Note that $\sqrt{2}\omega$ is the frequency of a single ball with a doubled spring constant.

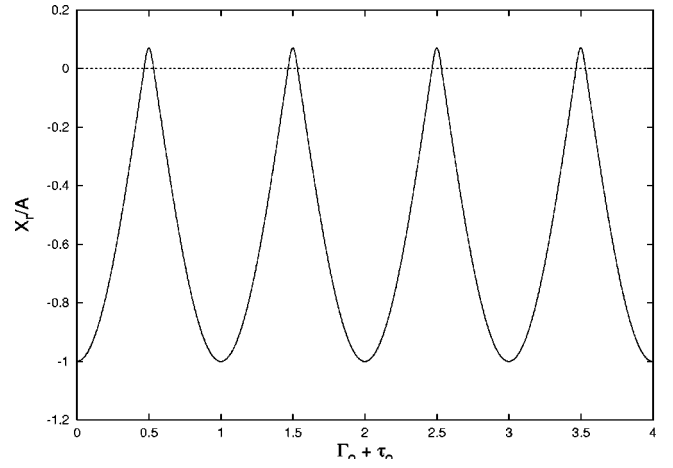


Fig. 6. Plot of the relative position X_r for the $N=2$ cradle as a function of time plotted in multiples of $\Gamma_0 + \tau_0$ (time between collisions+interaction time). The simulation was performed with a small ratio $K_r/K_c = 100$ to increase the collision time τ_0 .

To represent the resulting motion of the balls, it is helpful to switch identities after every collision, so that ball $1 \leftrightarrow$ ball 2 and thus $X_r \leftrightarrow -X_r$. We may then approximate X_r by

$$X_r = -A \cos \frac{\pi t}{\Gamma_0 + \tau_0}. \quad (13)$$

If we combine Eq. (13) with Eq. (10) for X_c , we find “beats” for the motion of one ball (with the above role reversal implied). For $\tau_0 \ll \Gamma_0$, we obtain

$$\hat{x} = -\frac{A}{2} \cos \frac{\pi t}{\Gamma_0} - \frac{A}{2} \cos \frac{\pi t}{\Gamma_0 + \tau_0} \approx -A \cos \frac{\pi t}{\Gamma_0} \cos \frac{\pi \tau_0}{2\Gamma_0^2} t, \quad (14)$$

where \hat{x} denotes that the identity switches between x_1 and x_2 after each collision. Thus, we have high-frequency oscillations with a frequency Ω which are modulated by the low-frequency $\pi \tau_0 / 2\Gamma_0^2 = \Omega^2 / 2\sqrt{2}\omega$.

We also can calculate the positions of the collisions. When they occur, we have $X_r = 0$, and the position of the collision is X_c . From Eq. (13), we obtain

$$\frac{\pi t_i}{\Gamma_0 + \tau_0} = \pi i + \frac{\pi}{2}, \quad (15)$$

where t_i is the time of the i th collision. Hence, the corresponding position is given by

$$x_i = X_c = -\frac{A}{2} \cos \left(\frac{\pi}{\Gamma_0} \left(i + \frac{1}{2} \right) (\Gamma_0 + \tau_0) \right) \approx \frac{A}{2} (-1)^i \sin \frac{\pi \tau_0}{\Gamma_0^2} t, \quad (16)$$

where we have used the definition of X_c in Eq. (10) and the approximation $\Gamma \gg \tau_0$. Figure 7 shows the excellent agreement between the analytical expression in Eq. (16) and our simulation.

The oscillation of the collision points for $N=2$ is caused by the finite elastic response of the balls. Plotting phase portraits at different times, as shown in Fig. 8, reveals the same characteristics we had obtained for the $N=5$.

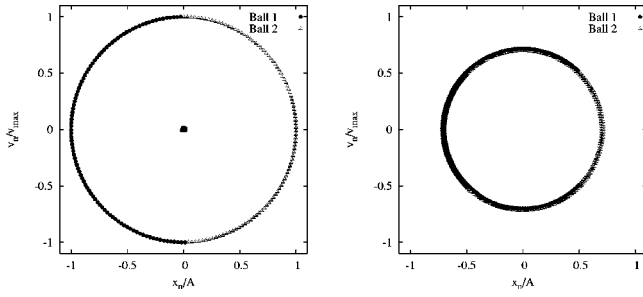


Fig. 7. Two phase portraits that characterize the motion of the $N=2$ cradle. The system slowly oscillates between the case where both balls move with the same speed, and the case where one ball collides with a stationary ball. The axes are made dimensionless by dividing the velocity of each ball by the maximum velocity of the incoming ball and the position by the initial amplitude.

V. THE EFFECTS OF DISSIPATION

Although the study of a dissipation-free version of Newton's cradle is interesting in its own right, any realistic simulation of the experiment needs to include dissipation. Two obvious such mechanisms are the velocity-dependent viscous drag of air and the viscoelastic dissipation associated with the collisions of the balls. We chose a simple linear dependence on the velocity $F_{fr} = \eta v$ (Stokes law).

The inelastic character of the collisions is modeled by including a viscoelastic dissipation force of the form¹⁶

$$F_{diss} = -\gamma \frac{d}{dt}(\xi^\beta), \quad (17)$$

into the equation of motion. Here, ξ is the overlap between two balls as defined in Eq. (3) and $\beta=3/2$ (Hertz–Kuwabara–Kono model).¹⁶

The equation of motion for the dissipative Newton's cradle is then given by

$$m\ddot{x}_n = k\xi_{n-1,n}^\alpha - k\xi_{n,n+1}^\alpha + k_g(x_{o,n} - x_n) - \eta v - \gamma \frac{d}{dt}(\xi^\beta). \quad (18)$$

The Stokes term continually removes energy from the system, while viscoelastic dissipation occurs only during collisions.

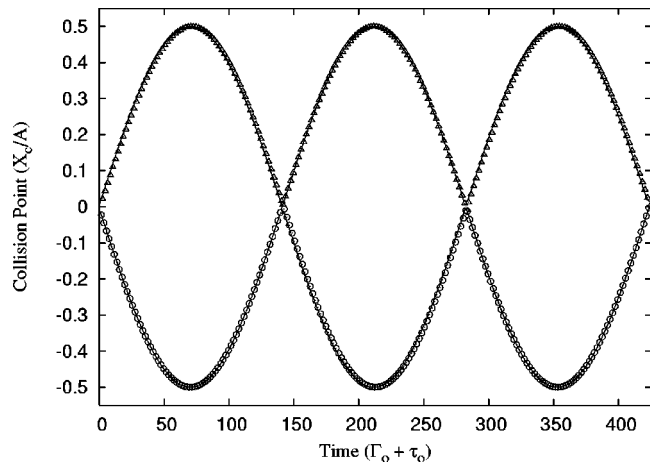


Fig. 8. For $N=2$, successive collisions take place in turn on the left (circles) and on the right (triangles) of the center of the system. The numerically determined points are well described by theory (continuous line), Eq. (16).

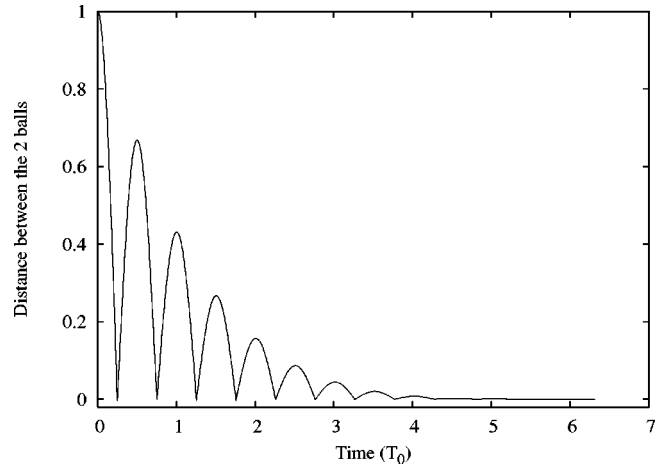


Fig. 9. Due to energy dissipation during the collisions, the distance between the centers of the balls decreases in time and the balls will swing in phase. The data are for $N=2$.

sions. Due to the velocity-dependent forces in the system, we utilize the Euler–Richardson method to solve the new equation of motion [Eq. (18)].¹² We use the same time step as for our dissipation free simulations. The value of the time step was tested using the Euler–Richardson method for the dissipation-free case and found to give excellent energy conservation.

To demonstrate the effect of the viscoelastic dissipation on the behavior of the system, simulations were run where the Stokes term was neglected ($\eta=0$). In Fig. 9, we plot the distance between the two balls as a function of time. This simulation demonstrates that the final collective motion of the balls that is reached experimentally is caused by the energy dissipation due to the collisions. The final amplitude of swing can be predicted in the following way.

Consider an N -ball cradle with initially only one ball moving with velocity v_0 . The total initial kinetic energy $S_0 = \frac{1}{2}mv_0^2$ may be written as the sum of the kinetic energy due to the motion of the center of mass S_c plus the kinetic energy relative to the center of mass, S_r ,

$$S_0 = S_c + S_r, \quad (19)$$

with $S_c = \frac{1}{2}Nm(1/N \sum_{i=1}^N v_i)^2$. Because all velocities are zero apart from $v_1 = v_0$, S_c reduces to $S_c = S_0/N$. From Eq. (19), we immediately obtain

$$S_r = \frac{N-1}{N} S_0. \quad (20)$$

Because all this relative kinetic energy will be dissipated in subsequent collisions, the final energy of the system is given by

$$S_{\text{final}} = S_0 - S_r = \frac{S_0}{N}. \quad (21)$$

The final energy of each ball, neglecting the Stokes term, is simply given by E_{initial}/N^2 . Note that this value is independent of the coefficient of dissipation, which specifies only the time it takes for the relative kinetic energy to be fully dissipated and, thus, the time it takes for all balls to swing in phase.

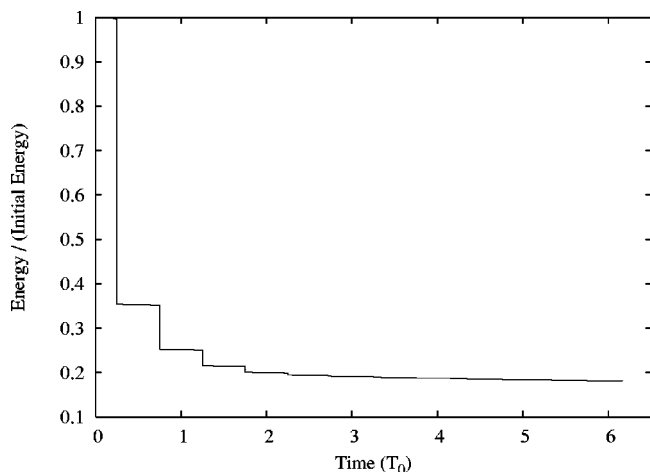


Fig. 10. Loss of energy due to the Stokes damping and viscoelastic dissipation for the $N=5$ cradle. The y axis is made dimensionless by dividing by the initial energy of the system.

For a finite value of η , the Stokes damping constantly removes energy from the system, causing the amplitude of all the balls to eventually diminish to zero. In Fig. 10, we show the variation of the total energy with time for a five-ball cradle where both Stokes damping and viscoelastic dissipation are included in the simulation. Here, we see that the energy decays quickly to approximately one-fifth of the initial energy, where the collective motion state is reached. It then continues to decay due to the Stokes damping.

VI. EXPERIMENTS

To examine the validity of our simulations, we have carried out experiments using a specially constructed large Newton's cradle consisting of four metal balls (diameter 6.8 cm, mass 0.7 kg) suspended from 1.3 m long wires. (The balls we used were commercial sand-filled metal boules.)

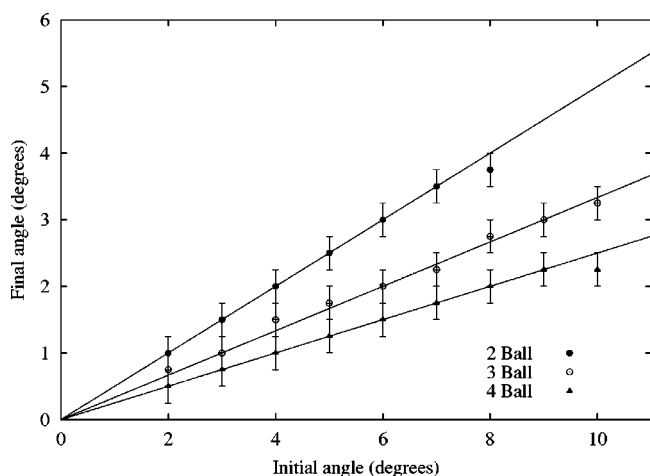


Fig. 11. Experimental data for Newton's cradle with $N=2, 3$, and 4 balls. A single ball is released from an angle θ_0 . After many collisions, the balls settle into a collective mode of motion where all move together with amplitude θ_c . The data is well described by $\theta_c = \theta_0/N$ (solid line). We take the error in the final angle of swing to be the accuracy of the protractors used, $\pm 0.25^\circ$.

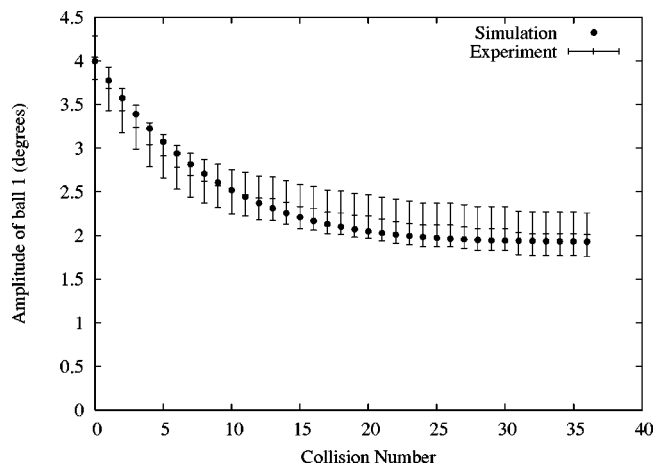


Fig. 12. Variation of the amplitude of ball 1 in a $N=2$ cradle with time. Shown are experimental data and results from our simulations. The experimental data in Figs. 12–15 are averaged over ten runs of the experiment, and the error in the amplitude is taken to be the accuracy of the angle measurement $\pm 0.25^\circ$.

Specially constructed large protractors were used for accurate measurements of the angle of swing to an accuracy of $\pm 0.25^\circ$.

Our first set of experiments investigated our prediction for the amplitude of the collective motion of the balls described in Sec. V. A single ball was released from an angle θ_0 onto a line of N balls. Once the state of collective motion was reached, we determined its amplitude θ_c . The time required for the system of balls to settle into the collective mode is between 1 and 2 min. This time compares with the time of about 1 h for the system to come to rest.

Figure 11 shows measurements of θ_c as a function of θ_0 for $N=2, 3$, and 4 . The data are well described by $\theta_c = \theta_0/N$, consistent with Eq. (21), and our conclusion that the collisions will only remove energy of the relative motion of the balls.

Our second set of experiments focused on energy dissipation due to the collisions of the balls. Again, a single ball was released from an angle θ_0 and collided with a line of 2, 3, or 4 balls. We determined its amplitude after every collision

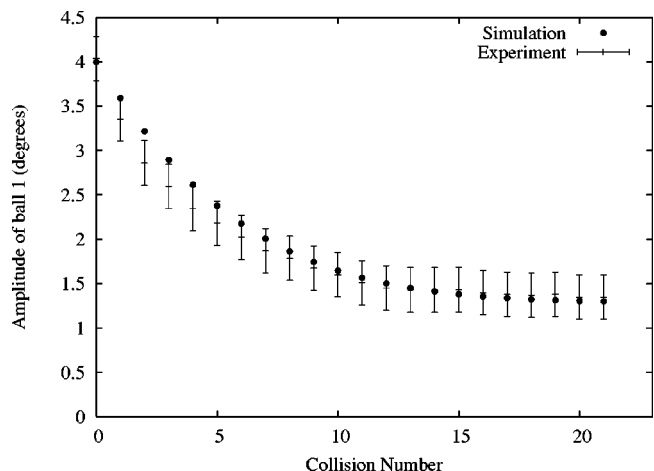


Fig. 13. Variation in amplitude of ball 1 for the $N=3$ cradle. The simulation used the same set of parameters as for the two-ball case.

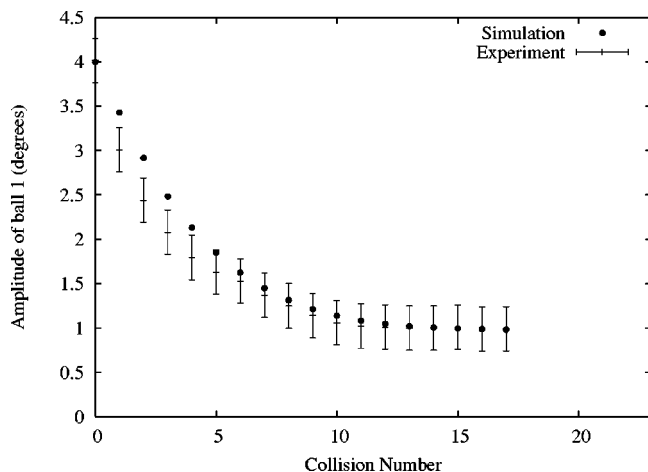


Fig. 14. Variation in amplitude of ball 1 for the $N=4$ cradle. The simulation used the same set of parameters as for the two-ball case.

with its neighboring ball. The experimental data, shown in Figs. 12–14, reveal that the textbook explanation of Newton’s Cradle with its prediction of a constant amplitude fails.

To determine a value for the damping constant η , the time-dependence of the amplitude was determined for a single ball and fitted to $\theta_{\max}(t) = \theta_0 \exp(-\eta t/2m)$ to give $\eta = 6.8 \pm 0.136 \times 10^{-4} \text{ kg s}^{-1}$. The constant k was calculated from Eq. (6) with $E = 2 \times 10^{11} \text{ Pa}$ and $\nu = 0.33$ for steel and was found to be $k = 1.38 \times 10^{10} \text{ kg m}^{-1/2} \text{ s}^{-2}$.

The viscoelastic dissipation parameter γ was then estimated by adjusting it in the simulation to match the dissipation seen in the two-ball experiment. The value was found to be $\gamma = 1.47 \times 10^2 \text{ kg s}^{-1} \text{ m}^{-2}$. This value was then used in the three- and four-ball simulations shown in Figs. 13 and 14.

We find from our simulations that the exact separation of the balls when a collision occurs has a very important influence on the behavior of the system. If balls 2–5 are initially in their exact equilibrium positions when they touch, the subsequent collisions will essentially be multiball collisions. In such collisions, the energy dissipated is less than in a series of two-ball collisions. However, any experimental setup has imperfections that will cause the system to deviate from this idealization, for example, small differences in the oscillation periods of the individual balls or the balls not hanging exactly at their equilibrium position.

To incorporate these imperfections into the simulation, we varied the value of k_g for each of the balls so that the periods of the balls vary slightly, and thus all collisions after the initial one are no longer multiball collisions. In Figs. 12–14, the periods of the balls vary by $\Delta T = 0.01 \text{ s}$ or $1/240$ th of a period. (This variation has no noticeable effect in the two ball case because all collisions are two-ball collisions.) When this effect is incorporated, we find good agreement between the simulations and the experimental data.

We have tested the effect of a range of differences in the periods of the balls. We found that there is little variation in the amplitudes obtained until we choose either very small values of ΔT that approach the idealized case, or large values of ΔT that no longer represent an accurate description of the experiment. We tested removing the multiball collisions by introducing very small gaps, Δx , between the balls in the simulation. For small values of $\Delta x \approx 0.1 \text{ mm}$, the amplitudes

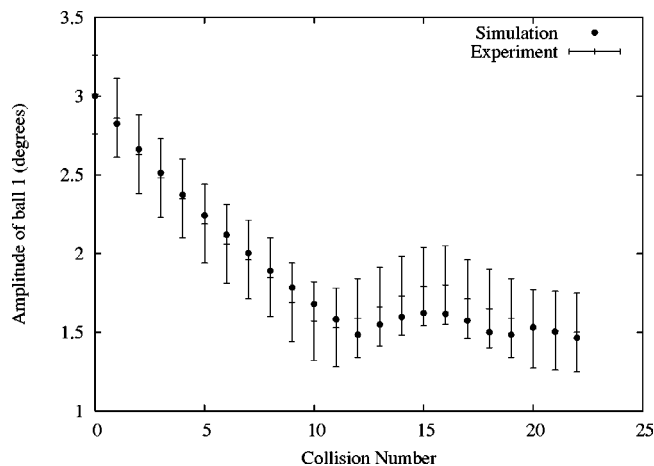


Fig. 15. Variation in amplitude of ball 1 for a $N=2$ cradle with a 1 mm gap between the rest positions of the balls. The simulation uses the same set of parameters as for the two-ball case of Fig. 12.

obtained in the simulations are almost identical to those obtained from the simulations that incorporate small variations in the period of the balls.

We also have considered the case where there is an appreciable gap between the balls. Figure 15 highlights the importance of a careful experimental setup, where instead of touching, there is a $\Delta x = 1 \text{ mm}$ gap between the balls when they are in their rest positions. Here, we see a “beating” effect where the amplitude of ball 1 does not simply decay, but oscillates. This behavior is well replicated by our simulation.

VII. CONCLUSION

We have shown that the physics involved in Newton’s cradle is far from trivial and that the standard textbook explanation is only a first approximation. In the context of physics education, our study of Newton’s cradle might fulfill two purposes. Students should see that apparently simple experiments, when closely examined, can raise a number of complicated questions. One also should be cautious about fully accepting well-established explanations of physical phenomena without carefully scrutinizing the arguments.

ACKNOWLEDGMENTS

This work was funded by Enterprise Ireland (Basic Research Grant No. SC/2000/239/Y) for one of the authors (S. H.) and a Trinity College Dublin Research Studentship for another (G. D.). The latter author (G. D.) would like to thank E. J. Hinch for detailed discussions of the problem and much advice.

^{a)}Electronic address: garyd@maths.tcd.ie

¹F. Bueche, *Principles of Physics* (McGraw–Hill, New York, 1986).

²M. Sternheim and J. Kane, *General Physics*, 2nd ed. (Wiley, New York, 1991).

³H. Ohanian, *Principles of Physics* (Norton, New York, 1994).

⁴E. Mazur, *Peer Instruction: A User’s Manual* (Prentice–Hall, N.J., 1997).

⁵A. B. Western and W. P. Crummett, *University Physics, Models and Applications* (Wm. C. Brown, Dubuque, IA, 1994).

⁶J. Wilson and A. Buffa, *College Physics*, 4th ed. (Prentice–Hall, Upper Saddle River, N.J., 2000).

- ⁷E. J. Hinch and S. Saint-Jean, "The fragmentation of a line of balls by an impact," *Proc. R. Soc. London, Ser. A* **455**, 3201–3220 (1999).
- ⁸F. Hermann and P. Schmäzle, "Simple explanation of a well-known collision experiment," *Am. J. Phys.* **49**(8), 761–764 (1981).
- ⁹F. Hermann and M. Seitz, "How does the ball-chain work?," *Am. J. Phys.* **50**(11), 977–981 (1982).
- ¹⁰M. Reinsch, "Dispersion-free linear chains," *Am. J. Phys.* **62**(3), 271–278 (1994).
- ¹¹V. Ceanga and Y. Hrmuzlu, "A new look at an old problem: Newton's cradle," *J. App. Math.* **68**, 575–583 (2001).
- ¹²H. Gould and J. Tobochnik, *An Introduction to Computer Simulation Methods: Applications to Physical Systems*, 2nd ed. (Pearson Education, 1996).
- ¹³L. Landau and E. Lifshitz, *Theory of Elasticity*, 2nd ed. (Pergamon, New York, 1970).
- ¹⁴D. Donnelly and J. Diamond, "Slow collisions in the ballistic pendulum: A computational study," *Am. J. Phys.* **71**, 535–540 (2003).
- ¹⁵An animation of the simulation can be downloaded from <http://www.maths.tcd.ie/~garyd/cradlevideo.html>.
- ¹⁶D. E. Wolf, "Modelling and computer simulation of granular media," in *Computational Physics*, edited by K. H. Hoffmann and M. Schreiber (Springer-Verlag, Berlin, 1996), pp. 64–95.



Thermoelectric Battery. At about the turn of the twentieth century, thermoelectric batteries were used to charge storage batteries. The circuit consists of a number of copper and bismuth wires, connected in series. All the copper-to-bismuth connections (for example) are gathered together and kept at one temperature, and the bismuth-to-copper junctions were kept at the other temperature. A gas burner placed in the center of the apparatus raises the temperature of the junctions collected at that point and the other junctions are kept cooler through the use of radiating fins. The overall EMF depends on the number of junctions. This piece of apparatus is at the physics department of Hobart and William Smith Colleges in Geneva, New York. (Photograph and notes by Thomas B. Greenslade, Jr., Kenyon College)